Microwave synthesis of single-crystalline perovskite Bi Fe O 3 nanocubes for photoelectrode and photocatalytic applications

Upendra A. Joshi, Jum Suk Jang, Pramod H. Borse, and Jae Sung Lee

Citation: Applied Physics Letters **92**, 242106 (2008); doi: 10.1063/1.2946486

View online: http://dx.doi.org/10.1063/1.2946486

View Table of Contents: http://scitation.aip.org/content/aip/journal/apl/92/24?ver=pdfcov

Published by the AIP Publishing

Microwave synthesis of single-crystalline perovskite $BiFeO_3$ nanocubes for photoelectrode and photocatalytic applications

Upendra A. Joshi, Jum Suk Jang, Pramod H. Borse, and Jae Sung Lee[a)]
Eco-friendly Catalysis and Energy Laboratory (NRL), Department of Chemical Engineering and School of Environmental Science and Engineering, Pohang University of Science and Technology, San 31 Hyoja-dong, Pohang 790-784, Republic of Korea

(Received 29 March 2008; accepted 22 May 2008; published online 18 June 2008)

A simple microwave synthesis procedure has been developed for the single-crystalline perovskite nanocubes composed of bismuth ferrite ($BiFeO_3$). Typical nanocubes had sizes ranging from 50 to 200 nm. The single-crystalline nature of nanocubes was confirmed by high resolution transmission electron microscopy and selected area electron diffraction pattern. X-ray diffraction pattern showed the rhombohedral phase with *R*3*c* space group. The material showed photoinduced water oxidation activity in both photoelectrochemical and photocatalytic modes. It could become a useful material for photoelectrode and photocatalytic applications. © *2008 American Institute of Physics*. [DOI: 10.1063/1.2946486]

Perovskite and related compounds are widely investigated because of their multiferroic, photocatalytic, and magnetic properties which are useful for applications in thin-film capacitor, nonvolatile memory, nonlinear optics, and photoelectrochemical cell.[1–4] Most perovskite phases are prepared by solid-state reactions between the corresponding oxides at temperature above 1000 °C. Recently, solution based methods have been widely developed for various perovskite nanomaterials sythesis.[5] Among the various classes of nanostructures, nanocubes have generated interest as potential building blocks in nanodevices and functional materials.

Bismuth ferrite ($BiFeO_3$) is an important multiferroelectric[6] and photocatalytic material. The synthesis of multiferroic nanostructures with a controllable size and shape is essential not only for smart device applications but also for fundamental studies.[7] Various procedures have been developed to synthesize $BiFeO_3$ nanostructure materials such as nanotubes, nanoparticles, and nanospindles. Park *et al.*[8] synthesized the $BiFeO_3$ nanotubes with alumina template. Han *et al.*[9] reported hydrothermal synthesis of bismuth ferrites with various morphologies. Similarly, Gao *et al.*[10] reported the synthesis of $BiFeO_3$ nanowires. It has been reported recently that the microwave synthesis methods could provide an efficient way to control phase selectivity as well as fast crystallization.[11] Komarneni *et al.*[12,13] reported the microwave-hydrothermal synthesis of $BiFeO_3$ at 194 °C for 2 h, but the product was highly crystalline agglomerated particles. Until now there is no other report of microwave synthesis of $BiFeO_3$ perovskite nanomaterials. By careful control of *p*H, temperature, and time of reaction, we were able to synthesize single-crystalline $BiFeO_3$ perovskite nanocubes.

Developing approaches to prepare perovskite nanomaterials in large scale has been the prime focus of our group. In this regards, we have previously reported the synthesis of perovskite $BaTiO_3$ and $SrTiO_3$ nanowires.[14–16] In this communication, we report a microwave synthesis of single-crystalline perovskite $BiFeO_3$ nanocubes. In short, 0.486 g (1 mmol) of $Bi(NO_3)_3.5H_2O$, 0.405 g (1 mmol) of $Fe(NO_3)_3.9H_2O$, 2.122 g (20 mmol) of Na_2CO_3, and 8.988 g (160.2 mmol) of KOH were added into 15.0 ml of distilled H_2O. The mixture was then transferred to a 125 ml Teflon reactor and placed in a microwave oven (Mars-5, CEM). The microwave reaction was carried out at 180 °C for 30 min.[17]

Figure 1 represents the synchrotron x-ray diffraction pattern of as-obtained microwave-synthesized product. All diffraction peaks of $BiFeO_3$ can be perfectly indexed by a rhombohedral phase with the space group *R*3*c* (No. 161).[18] The lattice parameters, refined with the Rietveld analysis, are $a=5.5501$, $b=5.5501$, and $c=13.7966$ Å as described in the supplementary material.[17] It is evident that the product is phase-pure, highly crystalline $BiFeO_3$. To investigate the morphology of the as-obtained product, we carried out scanning electron microscopy (SEM) analysis. As shown in Fig. 2(a), $BiFeO_3$ exhibits a well-defined cubic morphology with

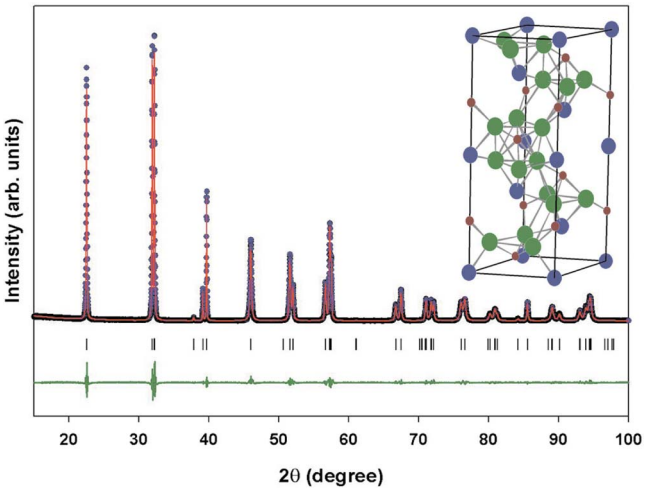

FIG. 1. (Color online) Observed (dots) and calculated (solid lines) diffraction patterns from the Rietveld analysis of synchrotron XRD data of $BiFeO_3$ nanocubes. The vertical tick marks shows the Bragg reflections. The trace in the bottom shows the difference plot of observed and calculated intensities. Inset shows the $BiFeO_3$, crystal structure (O as the largest spheres, Bi as medium-size spheres, and Fe as the smallest spheres).

[a)]Author to whom correspondence should be addressed. Tel: +82-54-279-2266. Fax: +82-54-279-5528. Electronic mail: jlee@postech.ac.kr.

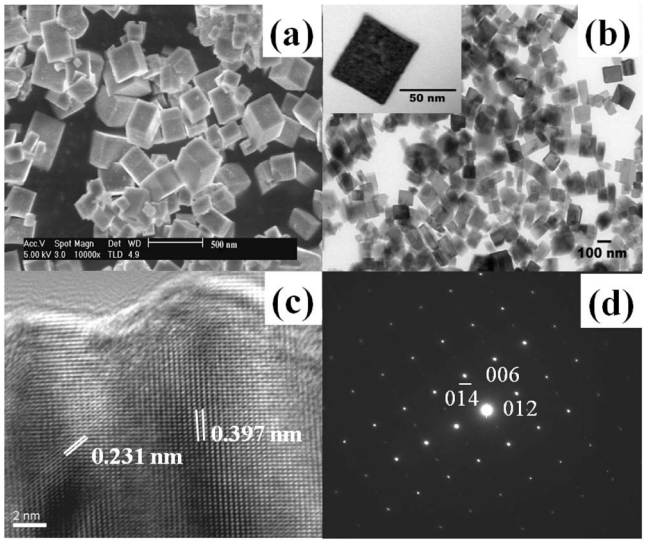

FIG. 2. (a) SEM image of $BiFeO_3$ nanocubes. (b) TEM image of $BiFeO_3$ nanocubes. Inset shows the TEM image of a single $BiFeO_3$ nanocube. (c) HRTEM image of a single nanocubes. (d) SAED pattern of the same crystal.

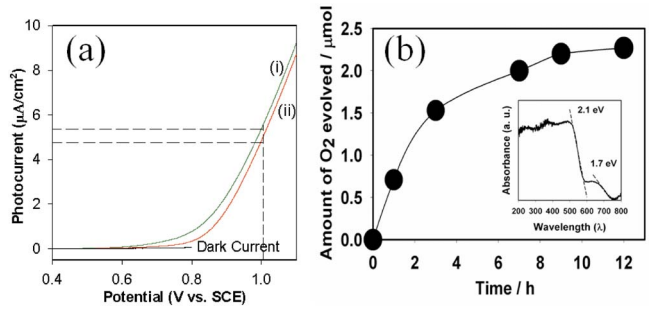

FIG. 3. (Color online) (a) Photocurrent density-potential curves of $BiFeO_3$ nanocubes (i) and $BiFeO_3$ bulk (ii) thin film electrodes under illumination. (b) Photocatalytic oxygen evolution under visible light irradiation over $BiFeO_3$ nanocubes. Photocatalysts (0.1 g): an aqueous iron chloride solution (4 mmol/l) 100 ml. Inset shows the UV-visible diffusion reflectance spectrum of $BiFeO_3$ nanocubes. Light source is a 500 W Hg lamp with a cutoff filter ($\lambda \geqslant 420$ nm).

an average size about 50–200 nm. We further examined the nanostructures with transmission electron microscopy (TEM) and high resolution TEM (HRTEM).

Figure 2(b) shows the typical TEM image of the $BiFeO_3$ nanocubes. The inset of Fig. 2(b) shows the high magnification TEM image of a single nanocube. Figure 2(c) shows a high resolution TEM micrograph of a $BiFeO_3$ crystal with clearly resolved interplanar distance $d_{012}=0.397$ nm and $d_{006}=0.231$ nm. The selected area electron diffraction (SAED) pattern in the inset of Fig. 2(d), taken along the [100] zone axis from an individual nanocubes shows sharp diffraction spots, indicating that the as-obtained $BiFeO_3$ nanocubes consists of single crystal. Moreover, the SAED patterns taken from different samples are found to be almost identical, which demonstrates that the entire sample consists of single crystalline nanocubes.

To gain further insight into the structural features of $BiFeO_3$ nanocubes, x-ray photoelectron spectroscopy (XPS) measurements were carried out. XPS spectra shown in supplementary material indicate that $BiFeO_3$ nanocubes consist of Bi, Fe, and O elements.[17] Further, the peaks at 711.2 and 724.7 eV correspond to Fe^{3+} while no peak due to Fe^{2+} can be found, which confirms that oxidation state of Fe is 3+ in $BiFeO_3$ nanocubes.[19] The peak at 529.5 eV corresponds to O^{2-} in the lattice.[20] Similarly, Bi 4*f* doublet of $BiFeO_3$ shows peaks at binding energies of 164.1 and 158.8 eV, characteristics of Bi^{3+}.[21]

$BiFeO_3$ is a small band gap metal oxide semiconductor useful for visible light active photocatalysis. The inset in Fig. 3 displays UV-visible spectrum of $BiFeO_3$ nanocubes that shows two absorption edges; the main edge at 2.1 eV and a shoulder at 1.7 eV. The band around 550 nm is due to metal-to-metal transition and the one around 700 nm is due to crystal field transition.[20] Gao *et al.*[10] studied the photoinduced oxidation ability of $BiFeO_3$ nanowires to produce O_2. Figure 3(a) shows the photocurrent generated by film photoelectrodes fabricated from $BiFeO_3$ nanocubes (i) and $BiFeO_3$ bulk (ii) materials, in water under visible light irradiation ($\lambda \geqslant 420$ nm). This represents a half-cell reaction of photoelectrochemical cells. It can be observed that the photocurrents generated from $BiFeO_3$ nanocube and bulk $BiFeO_3$ electrodes at 1.0 V versus SCE were approximately 5.2 and 4.7 $\mu A/cm^2$, respectively, while photocurrent was not generated under the dark condition.

We carried out the photocatalytic reaction in an aqueous $FeCl_3$ solution to check the O_2 production ability of as-obtained nanocubes. This represents a half-cell reaction of photocatalytic water splitting. The rate of oxygen evolution was measured from an aqueous solution containing 4 mM $FeCl_3$ as an electron acceptor under visible light irradiation ($\lambda \geqslant 420$ nm). The time course of oxygen evolution is shown in Fig. 3(b). During the initial reaction time (<3 h), the rate of oxygen evolution increased linearly. After 3 h of reaction time, the oxygen evolution approached saturation. This result can be attributed to the depletion of iron (III) chloride as an electron scavenger by the reduction reaction. Therefore, the initial rate of the oxygen evolution represents the photocatalytic activity of the material.

From our results, it could be considered that $BiFeO_3$ nanocubes would be a good candidate as a photoelectrode as well as a photocatalyst for oxygen evolution. Lou *et al.*[22] reported that $SrTiO_3$-coated $BiFeO_3$ nanoparticles can produce hydrogen in the presence of a hole scavenger under visible light. It means that $BiFeO_3$ based photoelectrode can simultaneously produce hydrogen and oxygen from water in the presence of the applied bias potential. UV-visible diffuse reflectance spectrum confirms that the $BiFeO_3$ nanocubes have a main absorption edge at ~600 nm, or an energy band gap of about 2.1 eV, consistent with a previous report.[23] In addition a secondary edge is observed at ~730 nm.[17] The sharp absorption edge confirms the high crystallinity of nanocubes.

In conclusion, we have synthesized $BiFeO_3$ nanocubes via simple microwave procedure. Typical size of nanocubes is in the 50–200 nm range. The procedure employs low cost raw materials yielding a phase-pure, single crystalline product. Photoinduced oxidation ability of $BiFeO_3$ cubes indicates that it could be a useful material for photoelectrode and photocatalytic applications. The procedure developed here can be useful for the synthesis of other perovskite nanomaterials.

This work was supported by the Hydrogen Energy R&D Centre, one of the 21st Century Frontier R&D Program and the Brain Korea 21 Program. U.A.J. thanks Dr. Namsoo Shin

of Pohang Light Source (PLS) 8C2 beamline for helpful discussion/analysis.

[1]T. Kimura, T. Goto, H. Shintani, K. Ishizaka, T. Arima, and Y. Tokura, Nature (London) **426**, 55 (2003).
[2]M. Zaleski, J. Appl. Phys. **87**, 4279 (2000).
[3]E. Nippolainen, A. A. Kamshilin, V. V. Prokofiev, and T. Jaskelainen, Appl. Phys. Lett. **78**, 859 (2001).
[4]P. H. Borse, U. A. Joshi, S. M. Ji, J. S. Jang, E. D. Jeong, H. G. Kim, and J. S. Lee, Appl. Phys. Lett. **90**, 034103 (2007).
[5]Y. Mao, T. J. Park, and S. S. Wong, Chem. Commun. (Cambridge) **46**, 5721 (2005).
[6]J. B. Neaton, C. Ederer, U. V. Waghmare, N. A. Spaldin, and K. M. Rabe, Phys. Rev. B **71**, 014113 (2005).
[7]X. Y. Zhang, C. W. Lai, X. Zhao, D. Y. Wang, and J. Y. Dai, Appl. Phys. Lett. **87**, 143102 (2005).
[8]T. J. Park, Y. Mao, and S. S. Wong, Chem. Commun. (Cambridge) **23**, 2708 (2004).
[9]J. T. Han, Y. H. Huang, X. J. Wu, C. L. Wu, W. Wei, B. Peng, W. Huang, and J. B. Goodenough, Adv. Mater. (Weinheim, Ger.) **18**, 2145 (2006).
[10]F. Gao, Y. Yuan, K. F. Wang, X. Y. Chen, F. Chen, and J. M. Liu, Appl. Phys. Lett. **89**, 102506 (2006).
[11]B. Vaidhyanathan, P. Raizada, and K. J. Rao, J. Mater. Sci. Lett. **16**, 2022 (1997).
[12]S. Komarneni, V. C. Menon, Q. H. Li, R. Roy, and F. Ainger, J. Am. Ceram. Soc. **79**, 1409 (1996).
[13]S. Komarneni, Q. H. Li, K. M. Stefansson, and R. Roy, J. Mater. Res. **8**, 3176 (1993).
[14]U. A. Joshi and J. S. Lee, Small **1**, 1172 (2005).
[15]U. A. Joshi, S. Yoon, S. Baik, and J. S. Lee, J. Phys. Chem. B **110**, 12249 (2006).
[16]U. A. Joshi and J. S. Lee, Solid State Phenom. **119**, 275 (2007).
[17]See EPAPS Document No. E-APPLAB-92-108824 for detailed synthesis procedure; details on XRD, photocatalytic and photoelectrochemical characterization; XPS analysis and UV-Vis spectrophotometery. For more information on EPAPS, see http://www.aip.org.pubservs/epaps.ht.
[18]JCPDS Card No. 86-1518.
[19]W. Eerenstein, F. D. Morrison, J. Dho, M. G. Blamire, J. F. Scott, and N. D. Mathur, Science **307**, 1203a (2005).
[20]S. T. Zhang, M. H. Lu, D. Wu, Y. F. Chen, and N. B. Ming, Appl. Phys. Lett. **87**, 262907 (2005).
[21]Y. H. Lee, J. M. Wu, Y. C. Chen, Y. H. Lu, and H. N. Lin, Electrochem. Solid-State Lett. **8**, F43 (2005).
[22]J. Luo and P. A. Maggard, Adv. Mater. (Weinheim, Ger.) **18**, 514 (2006).
[23]M. Tomkiewicz and H. Fay, Appl. Phys. **18**, 1 (1979).